Dynamic Contact Resistance of Series Spot Welds

Some effects of electrode force, current, and material surface condition on the dynamic resistance of spot welds are determined for different uncoated and galvanized auto-body steel combinations

BY W. F. SAVAGE, E. F. NIPPES AND F. A. WASSELL

ABSTRACT. A study of dynamic contact resistance was performed for series spot welds made with a 7/32 in. (5.56 mm) restricted-diameter, flat electrode and a 7/8 in. (22.2 mm) diameter flat copper stool. The effects of electrode force and material surface condition on the dynamic resistance at the sheet-to-sheet interface and the electrode-to-sheet interface for 0.035 in. (0.89 mm), uncoated, auto-body stock were investigated. Similar studies were performed both for welds made between two sheets of degreased galvanized steel and a dissimilar combination involving degreased galvanized steel welded to degreased-and-pickled, uncoated steel.

The shape of the curve for dynamic resistance as a function of time was found to differ markedly both with the surface condition of the stock and with different material combinations. Typical curves of dynamic resistance are presented for a variety of welding conditions, material combinations, and material surface conditions. The shape of each curve is explained by reference to tensile-shear strength data and metallographic studies of the individual welds.

Introduction

The quantity of heat generated at the faying surface of a resistance weld is proportional to the product of the square of the welding current, the resistance to the flow of current, and the time of current flow. The following relationship for the quantity of heat generated during the production of a resistance weld is often quoted in discussions of resistance welding:

$$H = kI^2Rt$$

where H = quantity of heat generated in calories; I = the RMS, or heating value of the welding current in amperes; R = the resistance in ohms; t = the weld time in seconds; k = a constant of proportionality.

This relationship is, however, an unfortunate oversimplification because the resistance varies in a complex fashion during the production of a weld and is a function of many interrelated factors including:

1. Electrode force (and follow-up characteristics).
2. Welding current.
3. Welding time.
4. Material characteristics.

Consequently, except in research laboratories where elaborate instrumentation is available, the actual quantity of heat involved in the production of a resistance weld is rarely evaluated. Therefore, the user of resistance welding has resorted to the traditional technique of qualifying a welding procedure on a particular machine and relying upon the inherent reproducibility of machine and control characteristics to make welds of consistently acceptable quality.

Unfortunately, reliable nondestructive means of ensuring weld quality have yet to be developed, and variables over which the operator has inadequate control often influence the reliability of production welds. The situation has been further complicated recently by the extensive application of resistance welding to the fabrication of galvanized steel and other materials where tip-pickup may cause comparatively rapid deterioration of the electrode surfaces and thus further impair weld reproducibility.

Recently, a number of electronic controls have been marketed which utilize, in one form or another, measurement of the dynamic variation in the resistance of the weld as a feedback signal. Certainly, the variation in dynamic resistance is intimately related to the progress of the welding operation. However, the published literature[1,2] provides only limited and inconclusive evidence as to the exact nature of the relationship.

The research described in this paper is the initial phase of an effort to provide a better understanding of the relationship between material and welding variables and the dynamic resistance changes. In a previous paper[3] the effects of material and welding variables on the static contact resistance, before and after welding, were reported for the series spot welding of 0.035 in. (0.89 mm) auto-body steel.

Object

The object of this investigation was to study the effects of welding current, electrode force, and initial surface condition on the changes in dynamic contact resistance during series spot welding of a 0.035 in. (0.89 mm) auto-body stock.

Material

The material employed in this inves-

W. F. SAVAGE is Professor of Metallurgical Engineering and Director of Welding Research, and E. F. NIPPES is Professor of Metallurgical Engineering, Rensselaer Polytechnic Institute, Troy, New York; F. A. WASSELL, formerly Research Fellow at Rensselaer Polytechnic Institute, is Manager, Welding Research, Armco Steel Corp., Middletown, Ohio.

tigation consisted of:

1. 0.035 in. (0.89 mm) thick mild steel auto-body stock, hereafter referred to as "steel."
2. 0.035 in. (0.89 mm) thick galvanized mild steel, with a 1.25 oz/ft² (0.38 kg/m²) commercial coating of zinc, hereafter referred to as "galvanized."

Typical chemical composition and mechanical properties of similar mild steel auto-body stock have been previously reported.[3,4]

Equipment

Welding

The resistance welding equipment employed in this investigation has been described in detail in previous papers.[3,4] A synchronous electronic welding control, adjusted to provide sinusoidal welding currents, was employed for controlling the weld time. The magnitude of the welding current was adjusted by varying the primary voltage supplied to the welding transformer.

Instrumentation

RMS and peak values of the secondary welding current were measured to ±3% using a commercially available portable secondary current meter.

Dynamic resistance measurements were computed from simultaneous displays of instantaneous voltage and current recorded photographically with the aid of a calibrated, 5 in. (12.7 cm), dual-beam, cathode-ray oscilloscope and a direct-developing camera. The oscilloscope had a DC sensitivity of 0.028 V/in. (0.011 V/cm) and essentially constant frequency response from DC to 30 kHz.

A voltage signal proportional to the instantaneous secondary current was obtained from a 9 microhm, water-cooled, manganin shunt in the secondary circuit. Leads for measuring the voltage drop in the weld were connected directly to the specimens with alligator clips.

Procedure

Welding

The measurements were conducted on different combinations of materials:

1. Steel-to-steel (as-received).
2. Steel-to-steel (degreased in tetrachlorethylene).
3. Steel-to-steel (degreased and pickled 2 min. in 50% HCl, water-rinsed, and dried).
4. Galvanized-to-galvanized (degreased).
5. Galvanized-to-degreased-and-pickled steel.

Preliminary welding tests were performed for each combination of material to establish the appropriate range of welding conditions for study. The following welding variables were maintained constant throughout the investigation: welding time—12 cycles (0.2 sec); electrode geometry (upper—7/32 in. (5.56 mm) restricted diam., flat face, lower—⅞ in. (22.2 mm) diam. flat Cu stool); electrode material—Cu-Zr (alloy recommended for galvanized[5]); specimen size—1 × 4 in. (2.54 × 10.16 cm); overlap—1 in. (2.54 cm).

Electrode forces of 300, 400, and 500 lb (136, 181 and 227 kg) and current values ranging from less than that required for sticking to beyond the expulsion limit were studied.

Dynamic Resistance Measurements

Oscillograms, photographed from the screen of the cathode-ray oscilloscope, were enlarged approximately five-fold; the instantaneous resistance values were calculated by dividing the instantaneous voltage by the instantaneous current, measured from the enlargements. Figure 1 illustrates typical oscillographic records of current and voltage as a function of time for steel-to-steel welds.

Testing

All welds were tested in tensile-shear using a conventional hydraulic tensile-testing machine; the maximum load was recorded as a measure of weld strength.

All welds were radiographed to detect any evidence of porosity or expulsion. Extra weld samples were produced at each combination of variables for subsequent metallographic examination at ×25 magnification.

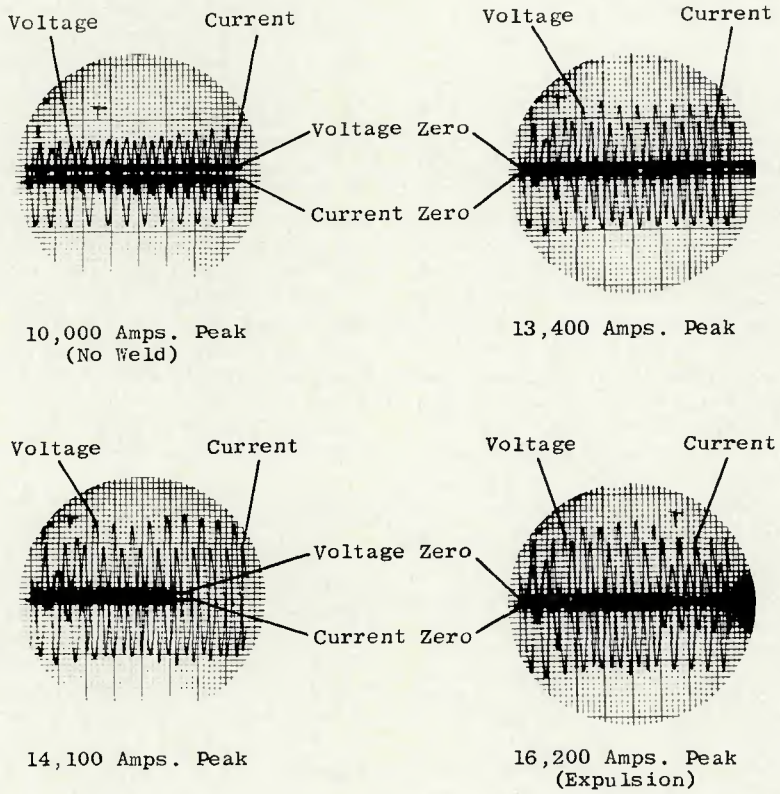

Fig. 1—Steel-to-steel oscillographic records of voltage and current

Dynamic Resistance Measurements for Steel-to-Steel Welds

Preparatory to conducting dynamic resistance studies, the influence of initial surface condition, material combination, and electrode force on the secondary current requirements was evaluated. Table 1 summarizes the acceptable range of RMS secondary currents for a weld time of 12 cycles with each combination of the above variables studied.

The minimum acceptable current was arbitrarily defined as that required to produce a weld with a tensile shear strength of 900 lb (408 kg). The maximum acceptable current was arbitrarily defined as that required to produce expulsion or spitting during welding. The average maximum value of tensile shear load sustained by the welds made with currents just below the expulsion limit is listed in each case in Table 1.

All dynamic resistance measurements were conducted with an electrode force of 400 lb (181 kg).

Initial Techniques

Initially, the dynamic resistance was measured 16 times during each ½ cycle of current flow at equally spaced instants of time. Table 2 summarizes a typical set of results for the first six ½ cycles of a 12 cycle weld. It is to be noted that the dynamic resistance changed but little during any single ½ cycle interval, as may be seen by inspection of the values in any one of the vertical columns in Table 2.

The greatest change in sheet-to-sheet resistance occurred at the beginning and end of the individual half cycles. However, the dynamic resistance over the 12 central increments of time changed by only a microhm or so during any given ½ cycle. Comparison of the average value within individual ½ cycle periods showed that a significant difference in dynamic resistance occurred between consecutive ½ cycles. This finding was confirmed by repeated experiments and permitted the use of the simplified experimental technique, described below, for the balance of the study.

Simplified Technique

Since the change in resistance within any individual ½ cycle interval was found to be small, the dynamic resistance was measured at the instant corresponding to the peak current value during each consecutive ½ cycle. Since the weld time was held constant at 12 cycles, this necessitated only 24 determinations of the dynamic resistance instead of 384 as were performed in the initial experiments. Thus, the simplified experimental procedure greatly reduced the time required to analyze the data and permitted studying more combinations of welding variables.

This technique further simplifies calculation of the dynamic resistance since at the peak current point $di/dt = 0$, and, therefore, the measured voltage drop is purely resistive. Thus no compensation for inductive reactance was necessary in the calculation. This eliminated the most time-consuming part of the initial technique.

Degreased-and-Pickled Steel-to-Steel Welds

In Figs. 2–5, the instantaneous resistance is plotted as a function of time in cycles for steel-to-steel welds made with degreased-and-pickled stock with increasing values of RMS secondary current.

At 7,070 A, as shown in Fig. 2, no welding occurred at the sheet interfaces, and the instantaneous contact resistance increased continuously from an initial static value of 8 microhms to 31 microhms during the 12-cycle weld time. This rise in resistance was undoubtedly due to a rise in temperature in the stock. Rectification, believed to occur as the result of oxide films present at the sheet interfaces, is indicated by the regular variation in instantaneous resistance that can be seen in alternate half cycles in Fig. 2. This effect decreased as the oxides gradually disperse with the rise in temperature at the interface.

Figure 3 shows data similar to that in Fig. 2, but for a secondary current of 8,550 A, which caused bonding of the steel sheets. The instantaneous resistance values increased more rapidly and reached a maximum of 35 microhms after approximately 6 cycles and then gradually dropped to 31 microhms at 9½ cycles. Following the decrease in resistance, a gradual rise to 33 microhms occurred during the remaining portion of the weld period.

The initial rapid rise in resistance in the first 6 cycles can be attributed to a rapid rise in the temperature, while the decrease in resistance after 9½ cycles in believed to coincide with the establishment of metal-to-metal contact across a major portion of the interface. Prior to this time it is probable that the individual metal-to-metal contacts initially present experienced an increase in size due to plastic flow of the hot metal at the interface. It is also likely that new metal-to-metal contacts were created during this interval until a substantial portion of the interface consisted of nearly complete metal-to-metal contact with a few entrapped oxides present. Some rectification was

Table 1—Range of RMS Welding Current for Acceptable Shear Strength; Weld Time—12 Cycles (0.2 Seconds)

Electrode force, lb	Min. current for 900 lb shear strength, A	Max. current (expulsion), A	Max. shear strength before expulsion, lb
Steel-to-Steel—Degreased:			
300	7,800	9,300	935
400	8,400	11,000	1,000
500	9,200	11,900	1,010
Steel-to-Steel—Pickled:			
300	9,300	10,000	930
400	10,200	12,700	1,030
500	10,600	14,100	1,110
Pickled Steel-to-Degreased Galvanized:			
300	11,300	13,800	1,170
400	11,800	14,400	1,200
500	13,200	16,200	1,220
Galvanized-to-Galvanized—Degreased:			
300	12,700	15,800[a]	1,260
400	13,300	17,200[a]	1,310
500	13,700	19,000[a]	1,310

[a] Electrode-to-sheet expulsion only.

Table 2—Variation in Instantaneous Resistance Within Each Half Cycle of Time for Steel-to-Steel Welds Made from Degreased-and-Pickled Stock

	Resistance, microhms					
Time interval	First half cycle	Second half cycle	Third half cycle	Fourth half cycle	Fifth half cycle	Sixth half cycle
1	12.7	9.2	35.4	19.5	14.6	15.9
2	12.9	9.1	24.4	26.3	20.2	21.4
3	14.4	10.4	23.1	30.0	23.8	23.5
4	14.2	10.8	24.0	34.0	28.6	24.3
5	14.4	11.9	26.1	36.5	27.7	26.5
6	13.9	12.1	26.2	36.8	28.2	27.1
7	13.3	12.1	26.2	37.7	28.2	27.1
8	12.8	12.5	26.3	37.6	28.0	26.5
9	12.7	12.7	26.2	37.5	28.0	26.5
10	13.0	13.5	27.4	37.2	27.8	26.4
11	14.0	13.8	30.9	36.7	28.1	26.1
12	13.0	14.3	34.0	36.0	27.3	26.6
13	14.3	14.9	29.7	36.1	24.6	28.3
14	13.8	15.1	26.9	34.1	20.2	28.0
15	13.9	15.4	24.5	33.3	15.5	27.9
16	15.8	14.1	16.8	31.4	—	28.3

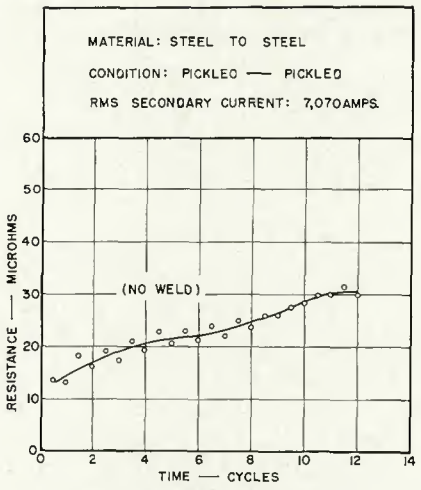

Fig. 2—Variation of instantaneous resistance with time for steel-to-steel welds made from degreased-and-pickled stock; 7,070 A

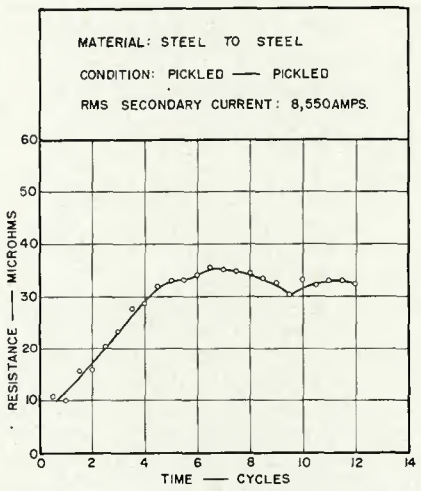

Fig. 3—Variation of instantaneous resistance with time for steel-to-steel welds made from degreased-and-pickled stock; 8,550 A

evident during the first few cycles of weld time.

A photomacrograph of the weld corresponding to the resistance-time plot in Fig. 3 is shown by Fig. 6A. Close inspection of the sheet-to-sheet interface revealed evidence of intimate contact between the sheets and the beginning of grain growth across the interface, but no evidence of melting can be detected. Metallographic evidence seems to corroborate the hypothesis proposed earlier that the dip in the resistance-time plot in Fig. 3 after 9½ cycles indicates the beginning of extensive plastic deformation of the metal at the sheet-to-sheet interface. However, it is not possible to rule out the beginning of localized melting at the interface as a contributing mechanism on the basis of present evidence.

In Fig. 4 similar data are shown for steel-to-steel welds made with degreased-and-pickled stock at 9,450 A. At this current, the instantaneous resistance values rose very rapidly to approximately 37 microhms at 4 cycles, decreased to 35 microhms at 5 cycles and then rose slightly to 36 microhms and remained at this value for the balance of the weld period. Note that the dip in resistance began after only four cycles with 9,450 A, as compared to the seven-cycle interval of rising resistance for the 8,550 A weld shown in Fig. 3. During the last 5 cycles of the weld period shown in Fig. 4, the resistance remained essentially constant, presumably because melting had occurred over a major portion of the interface. The temperature of the weld area increased rapidly during the last 5 cycles, and melting of the metal spread into the base metal as well as laterally along the interface.

The photomacrograph of the weld, for which the data of Fig. 4 were plotted, is shown in Fig. 6B. Examination of this photomacrograph reveals definite evidence of melting, as shown by the large columnar* grains extending from the center of the weld into the base metal. The location of the original sheet-to-sheet interface can still be detected at the left in the photomacrograph, and the fused zone

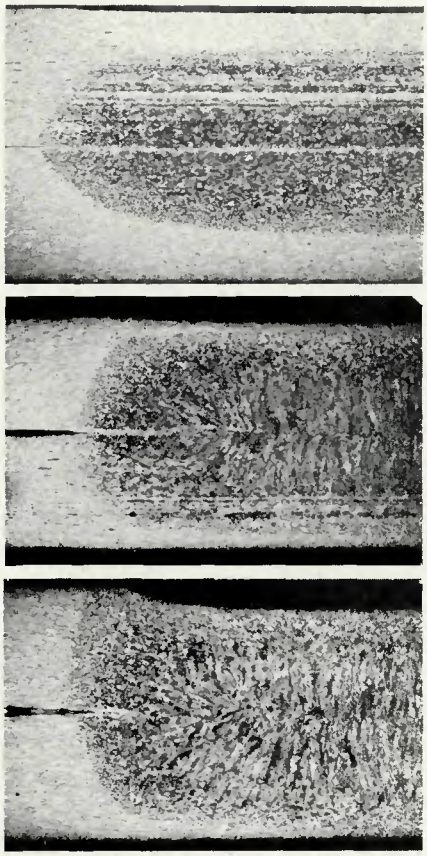

Fig. 6—Photomacrographs of steel-to-steel welds made from degreased-and-pickled stock, Nital etch, × 25 (reduced 28% on reproduction). RMS secondary currents in amperes as follows: A(top)—8,550; B(middle)—9,450; C(bottom)—11,400

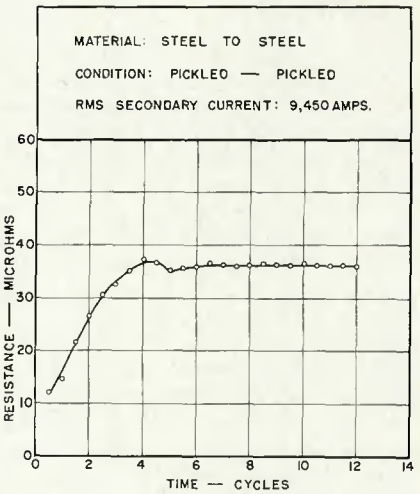

Fig. 4—Variation of instantaneous resistance with time for steel-to-steel welds made from degreased-and-pickled stock; 9,450 A

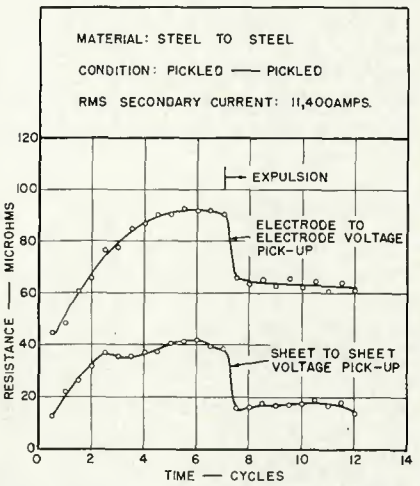

Fig. 5—Variation of instantaneous resistance with time showing expulsion for steel-to-steel welds made from degreased-and-pickled stock. Sheet-to-sheet and electrode-to-sheet voltage pick-up; 11,400 A

appears to be located symmetrically with respect to the interface.

Figure 5 (note change in the scale of resistance) shows resistance-time data for welds made from degreased-and-pickled steel stock with a current of sufficient magnitude to produce expulsion (11,400 A). For the lower curve, the sheet-to-sheet resistance rose rapidly during the first 2½ cycles, and

At higher magnifications, the typical columnar grains within the fusion zone of all welds exhibited a cellular-dendritic substructure characteristic of steel solidified rapidly in the presence of a steep temperature gradient at the solid-liquid interface. However, since the substructure is not evident at 25X, the grains in the fused zone will be referred to simply as columnar grains.

experienced a decrease during the third cycle (comparable to the dip in resistance observed in the fifth cycle for the weld made at 9,450 A shown previously in Fig. 4). The resistance then rose to a value of approximately 41 microhms, decreased gradually in the sixth cycle and then suddenly dropped to approximately 16 microhms in the seventh cycle. The resistance then remained substantially constant at 16 microhms for the remainder of the weld period.

The sudden drop in resistance was invariably observed in welds showing expulsion, and is believed to have resulted from the effective increase in contact area provided by the portion of the expelled metal trapped between the sheets. Increasing the weld current above the expulsion limit caused this sudden drop in contact resistance to occur earlier in the weld interval, as would be expected.

Figure 6C shows the fusion zone of the weld corresponding to the data shown in Fig. 5. The weld exhibits large columnar grains in the fused zone, and the excessive indentation of the top sheet is characteristic of welds in which expulsion has occurred.

The upper curve in Fig. 5 was made at the identical current of 11,400 A, but the resistance was measured from electrode-to-electrode instead of from sheet-to-sheet. Essentially, the only differences to be noted between the two curves are the higher resistance values and the lack of the characteristic dip in resistance early in the weld period when the resistance is measured from electrode to electrode. The additional resistance contributed by the two electrode-to-sheet interfaces and the body resistance of the stock appears to mask the characteristic dip in resistance at the beginning of bonding. Attention is called to the fact that the sharp drop in resistance began in the seventh cycle and that the resistance dropped 25 microhms in ½ cycle in both of the curves shown in Fig. 5, although the data were obtained from two different welds.

As-Received Steel-to-Steel Welds

Figures 7-9 show the instantaneous resistance as a function of time for steel-to-steel welds made with as-received stock. The static contact resistance of the material in this condition was extremely high and erratic, ranging from 97 to 3,700 microhms.

At 5,850 A, the first noticeable bonding action was observed between a pair of specimens with an initial contact resistance of 450 microhms. As can be seen from examination of Fig. 7, the instantaneous resistance dropped from 450 to approximately 58 microhms within the first half cycle, then

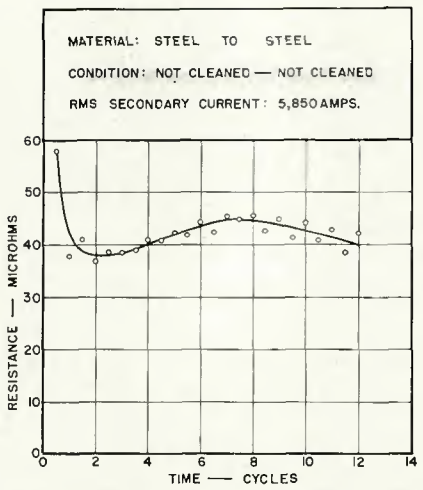

Fig. 7—Variation of instantaneous resistance with time for steel-to-steel welds made from as-received stock; 5,850 A

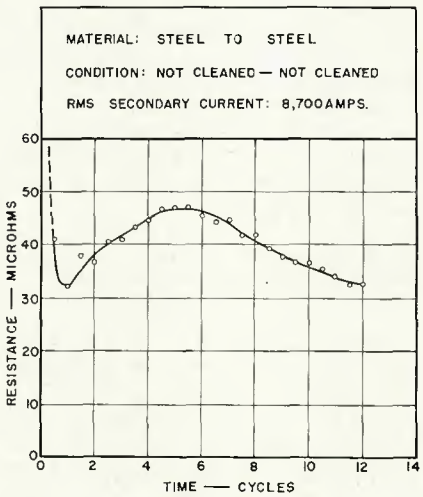

Fig. 8—Variation of instantaneous resistance with time for steel-to-steel welds made from as-received stock; 8,700 A

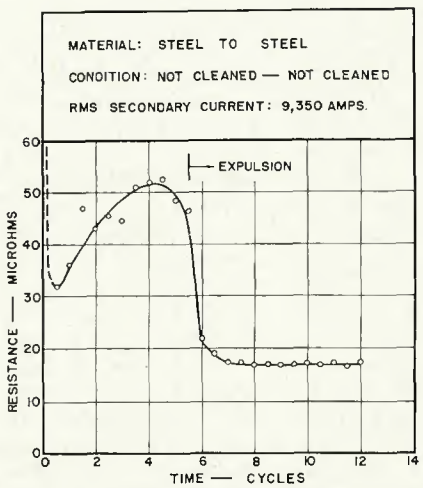

Fig. 9—Variation of instantaneous resistance with time showing expulsion for steel-to-steel welds from as-received stock; 9,350 A

continued to drop more gradually to a minimum of 38 microhms at the end of 2 full cycles. The resistance then rose to a maximum value of 45 microhms after 7 cycles and then decreased to 40 microhms by the twelfth cycle.

This complex behavior is typical of welds made in as-received uncoated steel with a high initial surface-contact resistance. It should be noted that the dynamic resistance values shown in Fig. 7 for steel in the as-received condition are generally higher than corresponding values previously presented in Fig. 3 for an equivalent weld in degreased-and-pickled steel. Evidence of rectification can be seen in the data of Fig. 7 throughout all 12 cycles, possibly as a result of the presence of more persistent oxides at the interface. Note also that the characteristic dip in resistance, discussed previously in connection with welds in degreased-and-pickled stock, is not evident.

In Fig. 8 for a weld made using 8,700 A, the initial static contact resistance of 97 microhms decreased to a minimum of 33 microhms within the first cycle of weld time. The instantaneous resistance then increased to a maximum of 47 microhms and then fell again to 33 microhms at the end of the weld period. The latter decrease in resistance appears to coincide with the growth of the fused zone.

Figure 9 shows similar data for a weld made at 9,350 A and illustrates the effect of expulsion on the resistance of a weld in as-received stock. The initial static contact resistance of 1600 microhms dropped very rapidly in the first half cycle to 32 microhms, and rose to a peak value of 52 microhms after 4 cycles. The resistance then decreased gradually until the sixth cycle, when, as expulsion occurred, the resistance dropped suddenly to 17 microhms, and remained constant for the duration of the weld.

Measurements for Galvanized Welds

Degreased-and-Pickled Steel to Degreased Galvanized Welds

Figures 10 and 11 show similar data for degreased-and-pickled steel welded to degreased galvanized stock. In Fig. 10, for a weld made at 12,900 A, the initial resistance of 30 microhms decreased to a value of 8 microhms by the end of the third cycle. The resistance fluctuated slightly until the seventh cycle and then gradually increased to 19 microhms during the final 5 cycles of the weld period.

This type of resistance-time curve is typical for welds made between degreased-and-pickled steel and degreased galvanized steel whenever the

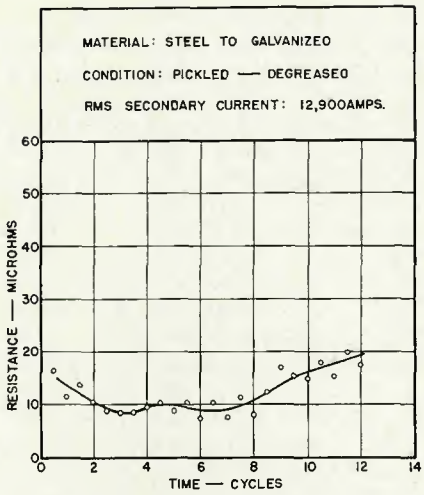

Fig. 10—Variation of instantaneous resistance with time for steel-to-galvanized welds made from degreased-and-pickled steel and degreased galvanized stock; 12,900 A

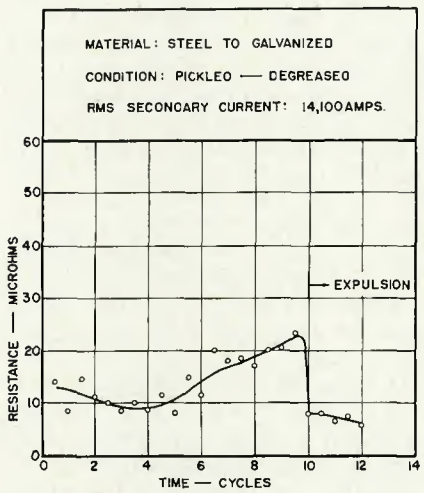

Fig. 11—Variation of instantaneous resistance with time showing expulsion for steel-to-galvanized welds made from degreased-and-pickled steel and degreased galvanized stock; 14,100 A

zinc at the interface melted and dispersed, allowing the formation of a steel-to-steel fused zone. The decrease in resistance noted in the first 3 cycles may be attributed to the improved metal-to-metal contact at the interface caused by the melting of zinc, and the rise in resistance in the last 5 cycles is believed to be due to the dispersal of the zinc and the rapid rise in temperature accompanying the melting of steel at the interface.

A photomacrograph of a similar weld made with 12,300 A is shown in Fig. 12A. This weld still shows evidence of zinc entrapped between the steel slightly to the right of the original unbonded interface at the left. A few columnar grains can be seen at the right side of the photomacrograph, indicating the beginning of melting of the steel.

A photomacrograph of the weld corresponding to the data in Fig. 10 is shown in Fig. 12B. Examination confirms the fact that the melting of steel occurred, as indicated by the columnar grains in the fused zone. The original interface with the dark-etching zinc coating can still be seen at the left side of this photomacrograph.

Figure 11 is a resistance-time plot for a degreased-and-pickled steel-to-degreased-galvanized-steel weld exhibiting expulsion, made at 14,100 A. The decrease in resistance typical of the melting of the zinc can be seen during the first 3 cycles and is followed by a rise in resistance during the next 7 cycles. The resistance dropped sharply during the tenth cycle when expulsion occurred and the resistance then remained at a low value for the remainder of the weld period.

Figure 12C shows the weld from which the data were obtained for Fig. 11. Attention is called to the large columnar grains and to the fact that the fused zone is displaced relative to the original location of the interface in the direction of the bare steel sheet. Excessive indentation of the degreased-and-pickled steel may also be observed at the top of the macrograph.

Degreased Galvanized-to-Galvanized Welds

The variation of instantaneous resistance with time for degreased galvanized-to-galvanized welds is shown in Fig. 13. The upper curve of Fig. 13 shows the resistance-time relationship for a welding current of 6,340 A.

Although no bonding occurred at the sheet-to-sheet interface, the resistance decreased from 21 to 13 microhms in the first 1½ cycles. The resistance then increased to 21 microhms in the next 4 cycles, and subsequently decreased to 14 microhms during the last 6½ cycles.

The drop in resistance early in the weld period may be similar to the effect observed in the as-received steel-to-steel welds shown in Figs. 7–9 where the high initial contact resistance was observed to decrease rapidly in the first cycle. However, the form of the curve gradually changed from that observed in the upper curve to that shown in the lower curve of Fig. 13 as the welding current was increased to 13,900 A. The gradual decrease in resistance after the second cycle to 3 microhms at the end of the weld was characteristic of degreased galvanized-to-galvanized whenever fusion occurred at the sheet-to-sheet interface. The slight rise in resistance during the first 1½ cycles seemed to be associated with heating prior to melting of the zinc at the sheet-to-sheet interface.

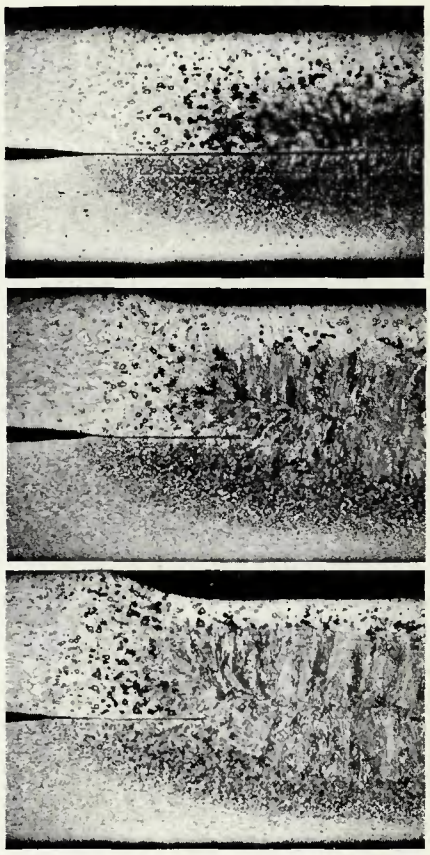

Fig. 12—Photomacrographs of steel-to-galvanized welds made from degreased-and-pickled steel and degreased galvanized stock, Nital Etch, × 25 (reduced 28% on reproduction). RMS secondary currents in amperes as follows: A(top)—12,300; B(middle)—12,900; C(bottom)—14,100

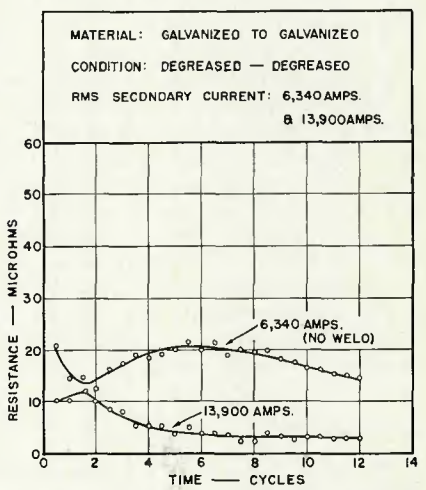

Fig. 13—Variation of instantaneous resistance with time for galvanized-to-galvanized welds made from degreased stock

Figure 14A shows a weld made with 9,200 A. This value of current was just sufficient to fuse the zinc at the sheet-to-sheet interface, but no melting of the steel or any evidence of steel-to-steel contact can be observed.

A photomacrograph of a weld made at 13,300 A appears in Fig. 14B. A thin layer of zinc was still visible between the sheets, but upon examination traces of steel-to-steel contact across the interface were found in some regions of the original weld. Some melting of steel had occurred as evidenced by the presence of columnar grains, but complete mixing of the zinc coating with the steel did not occur.

A photomacrograph of the weld made at 13,900 A, corresponding to the lower curve of Fig. 13, is shown in Fig. 14C. Evidence of the formation of a steel fused zone is afforded by the columnar grains in the steel at the interface. Zinc is visible at the interface between the sheets at the left, extending for some distance from the edge of the fused zone. The indentation of the top sheet is excessive, and a small surface crack is visible in the original macrograph at the top surface, just beneath the original location of the upper electrode. It should be noted that the currents employed in producing the welds in Figs. 14B and 14C differed by only 600 A, indicating the critical nature of the resistance welding of galvanized stock.

Shear Strength of Degreased Galvanized-to-Galvanized Welds

A typical curve of shear strength as a function of welding current for galvanized-to-galvanized welds made from degreased stock is illustrated in Fig. 15. A transition point, observed at a welding current of 13,600 A, coincides with the beginning of steel-to-steel contact at the interface of the weld. Below the transition current a layer of zinc was observed to separate the steel at the interface (as shown in Fig. 14B), while above the transition current, steel-to-steel contact was observed (as shown in Fig. 14C).

Obviously, the strength of the weld up to this point is entirely dependent upon a zinc-to-zinc weld. As the welding current was increased above the transition point, the area of the steel-to-steel contact across the interface was observed to increase as zinc was squeezed out of the weld area, although some zinc probably remains as an iron-zinc alloy or an intermetallic compound. This observation was confirmed repeatedly, both by metallographic evidence and by an increase in the size of the fused zone torn from the sheet during testing.

As may be noted in Table 1, the galvanized steel welds exhibit approximately 30% greater tensile shear strength than those in bare steel. This increase in strength results from the zinc braze surrounding the fused zone.

Conclusions

1. The dynamic contact resistance was found to remain essentially constant within the individual half-cycle intervals of a 12 cycle weld, and therefore, for the majority of cases, the dynamic resistance was determined only at those instants during each consecutive half cycle corresponding to the peak of the current waveform.

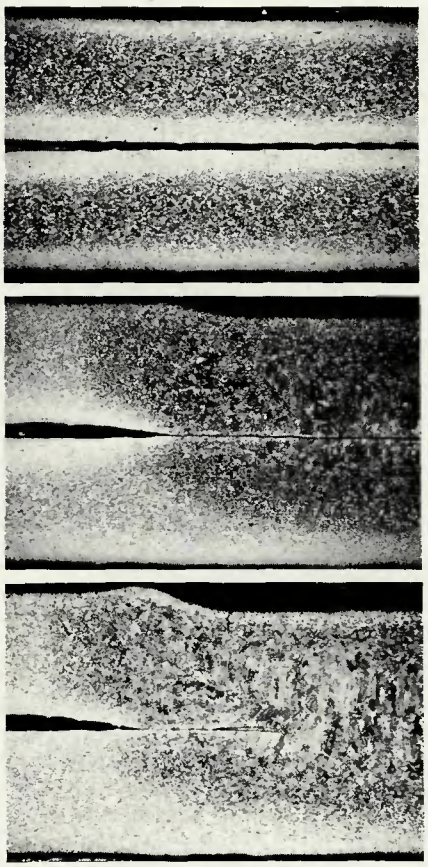

Fig. 14—Photomacrographs of galvanized-to-galvanized welds made from degreased stock, Nital etch, × 25 (reduced 28% on reproduction). RMS secondary currents in amperes as follows: A(top)—9,200; B(middle)—13,300; C(bottom)—13,900

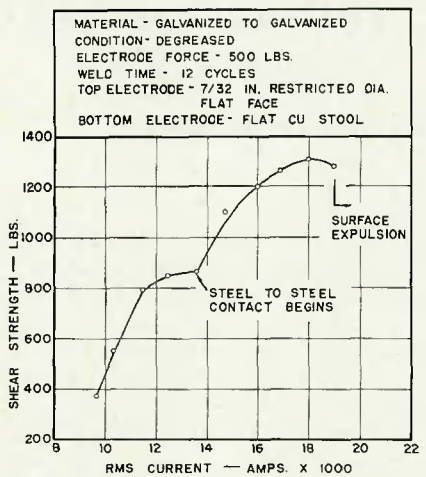

Fig. 15—Shear strength of galvanized-to-galvanized welds made from degreased stock showing a typical transition point in the curve

2. For degreased-and-pickled, steel-to-steel welds, with a welding current of 7,070 A RMS, the dynamic resistance at the weld interface increased from 8 to 30 microhms in a continuous fashion and no welding occurred.

3. Under optimum welding conditions with degreased-and-pickled steel stock, the dynamic resistance at the sheet-to-sheet interface rose to a maximum of approximately 35 microhms, experienced a slight decrease, then rose again to about 35 to 40 microhms and remained essentially constant. The slight dip appeared to correspond to the beginning of melting at the weld interface.

4. The maximum dynamic resistance, and the subsequent characteristic dip in the dynamic resistance, both occurred earlier in the weld cycle as the welding current was increased.

5. Whenever expulsion occurred in degreased-and-pickled steel, a sharp drop in contact resistance to a low stable value was observed at an instant corresponding to the beginning of expulsion for all material combinations studied.

6. The sharp drop, characteristic of the beginning of expulsion, occurred earlier in the cycle as the welding current was increased above the expulsion limit.

7. With steel-to-steel welds in as-received stock, the dynamic resistance invariably decreased to a minimum value of approximately 30 to 40 microhms within the first 1 to 2 cycles of the 12 cycle weld time, increased to a maximum of 45 to 50 microhms at a rate which increased with increasing welding current, and then decreased again.

8. After the maximum dynamic resistance of 45 to 50 microhms was experienced with as-received, uncoated, auto-body stock, the dynamic resistance experienced a gradual decrease of 30–35% under optimum welding conditions, a gradual decrease of 0–20% when no welding occurred, and a precipitous decrease of 60–70% when expulsion occurred.

9. With degreased-and-pickled steel and degreased, galvanized stock, the dynamic resistance was observed to decrease to a minimum and then rise again during a weld made under optimum conditions.

10. With currents just below the lower limit for welding degreased galvanized steel, the dynamic resistance decreased to a minimum of 14–15 microhms, increased to a maximum of 20–25 microhms, and then decreased gradually by approximately 30% to 14–15 microhms. Thus, a dynamic resistance curve for a com-

pletely unsatisfactory weld in galvanized stock was found to have the same general shape as that for a weld made in uncoated steel under optimum conditions.

11. The dynamic resistance curve for satisfactory welds in degreased galvanized stock was observed to decrease to a value of about 10 microhms in the first half-cycle, rise to a value of about 12-14 microhms, and then fall gradually to a constant value of 3 to 4 microhms.

12. The usual precipitous drop in dynamic resistance corresponding to the beginning of expulsion was never observed with galvanized stock, since spitting at the electrode-to-sheet interface occurred below the sheet-to-sheet expulsion limit.

13. The strength-current characteristic for galvanized-to-galvanized welds was found to exhibit a pronounced transition at approximately 830 lb (375 kg) and 13,600 A. Metallographic studies indicated that this break corresponds to a transition from bonding by melting of the zinc coating to the production of a fused zone between the underlying steel sheets.

Acknowledgments

The authors wish to acknowledge the financial support provided by the Welding Research Council for the performance of the work described in this report. The authors also wish to acknowledge the guidance and council provided by the members of the Series Spot Welding Sub-Committee of the Resistance Welding Research Committee.

References

1. Roberts, W. L., "Resistance Variations During Spot Welding," *Welding Journal, 30* (11), Nov. 1951, pp. 1004 to 1019.

2. Van Sciver, H. D., "Spot Weld Monitoring by Resistance Change," Electric Arc and Resistance Welding III, Oct. 1952, pp. 101-113, published by A.I.E.E., New York, N. Y.

3. Savage, W. F., Nippes, E. F., and Wassell, F. A., "Static Contact Resistance of Series Spot Welds," *Welding Journal,* 56(11), Nov. 1977, Research Suppl., pp. 365-s to 370-s.

4. Nippes, E. F., and Domina, F. H., "Series Spot Welding of 0.036 Inch Auto-Body Steel," *Welding Journal, 33* (10) Oct. 1954, Research Suppl. pp. 535-s to 544-s.

5. AWS Welding Handbook, Sixth Edition, Section 2, 1969, pp 28-29.